

# Molecular Modelling of Some Ligands Against Acetylcholinesterase to Treat Alzheimer's Disease

Şaban KALAY<sup>1\*</sup> , Hatice AKKAYA<sup>1</sup> 

<sup>1</sup>Division of Biochemistry, Department of Basic Pharmaceutical Sciences, Faculty of Pharmacy, University of Health Sciences, 34668 Istanbul, Türkiye

\*Corresponding Author. E-mail: [saban.kalay@sbu.edu.tr](mailto:saban.kalay@sbu.edu.tr) (S.K.); Tel. +90 553 002 21 90

Received: 22 September 2023 / Revised: 04 October 2023 / Accepted: 04 October 2023

**ABSTRACT:** Many molecular modeling methods have been used for the discovery of new drugs and compounds. Human acetylcholinesterase (AChE), an important target for therapeutic drugs, is docked with AutoDock Vina software embedded in the UCSF Chimera, together with current drug ligands used in the treatment of Alzheimer's disease and phytochemicals that slow the onset and progression of the disease. Considering protein ligand interactions, affinities and molecular properties, the variance map of the simulated quercetin-AChE complex yielded reasonable results with the molecular dynamics simulation program iMod server, and it can be said that this structure has the potential to act as an inhibitor.

**KEYWORDS:** Acetylcholinesterase; Alzheimer; molecular docking; molecular dynamics simulation; quercetin.

## 1. INTRODUCTION

Alzheimer's Disease (AD) is the most common cause of adult-onset dementia, which continues with a decline in cognitive function with behavioral symptoms. It contains acetylcholinesterase (AChE) licensed for the symptomatic treatment of AD as well as plant-derived molecules where AChE/butyrylcholinesterase (BChE) inhibitors (physostigmine and huperzine A) are effective in cognitive disorders. These drugs constitute 80% of commercially available drugs [1].

Tacrine, one of the first AChE inhibitors (AChE-Is) is no longer used in the treatment of AD due to its hepatotoxicity. Currently available AChE-Is are rivastigmine, galantamine and donepezil. The efficacy of the three AChE-Is is similar but the benefits are slight. Despite the limited activity of AChE-Is, these drugs are still a pharmacotherapeutic resource for the treatment of AD. Another approach to investigating AChE-Is is their use in combination with other drug classes such as antioxidant agents [2]. It has been reported that the intake of phytochemicals regulates the antioxidant system, cognitive and physical performance and improves health status by increasing neuronal cell survival. Studies have shown that polyphenols can play an important role in improving the neurodegenerative disease process [3].

Bioinformatics has a very important role in the study of targets and compounds for the treatment of a disease. Computational docking can be used to discover drugs through protein-ligand interactions. Molecular dynamics simulation has attracted attention for revealing the binding mechanism and conformational behavior of proteins and potential inhibitors [4,5]. Recently conducted molecular dynamics simulation studies of the AChE enzyme are often modeling and examining the mechanisms of binding of chalcones, piperazines, tacrine, coumarin, tyrosol, and naphthalene derivatives to the AChE protein [6-15]. In silico modeling studies have been conducted to investigate the effects of chalcone derivatives containing quinoline on Alzheimer's disease [6]. They stated that two of the compounds they tested significantly inhibited AChE and BChE isoenzymes. Due to their satisfactory ADME profiles, these candidate molecules have been suggested as oral drug models. In another study, the inhibitory property of a ligand with drug bank code DB00983 on human AChE enzyme was discovered using molecular dynamics simulations [7]. In another study, 2-furoic piperazide derivatives were synthesized and their potential inhibitory effects on  $\alpha$ -glucosidase, AChE, and BChE enzymes were investigated [8]. The molecule was suggested to be an inhibitor of AChE and BChE, based on the results of the study and their bioactivity potentials were supported by molecular docking studies [8]. In another study, the potential inhibitory effects of tacrine derivatives on the AChE (1ACJ) and BChE (4BDS) enzymes were analyzed using alignment-independent 3D-QSAR with the Pentacle software. The statistical results and

**How to cite this article:** Kalay Ş, Akkaya H. Molecular Modelling of Some Ligands Against Acetylcholinesterase to Treat Alzheimer's Disease. J Res Pharm. 2023; 27(6): 2199-2209.

predicted pIC<sub>50</sub> values were found to be promising [9]. In a study where 4-aryl-substituted-4H-pyran derivatives were synthesized it was suggested that these compounds could be used for the treatment of Alzheimer's, Parkinson's and Autism [10]. A synthetic compound derivative of kumarin and 4-aryl-kumarin has been reported to have a promising AchE inhibitory activity with an efficacy rate of 68.54% [11]. The modeling studies indicate that compounds with a small ring size, a higher number of -CH<sub>2</sub>- groups, a higher number of secondary aromatic amines, and a higher number of aromatic ketone groups may be better AchE inhibitors [12]. The triazolic analogues of tyrosol are reported to competitively inhibit AchE [13]. In a study, it has been reported that different naphthalene derivatives significantly reduce the levels of AchE in mouse brains [14]. In the virtual scan, known acetylcholinesterase inhibitors (rivastigmine, galantamine and tacrine) as well as some phytochemicals (quercetin, genistein and some flavonoids) were selected. Applied in silico approaches will provide new information to identify and develop new drug development inhibitors [15].

## 2. RESULTS AND DISCUSSION

AchE is a very important hydrolase involved in the regulation of neurotransmission in the entire nervous system. Any deformation that occurs in synaptic transmission is conspicuous for the control of AD. Therefore, cholinesterase inhibitors have been widely studied as therapeutic agents in this disease [16, 17]. Although more than 100 AchE crystal structures are known today only the human AchE crystal structure is known in detail due to difficulties in crystallization of the protein [18,19]. The structure of human AchE in complex with donepezil is a dimeric protein with two independent asymmetric units (Figure 1. a). Amino acids Y337, Y341, W286, F295, S203, E202, W86 and H447 produce inhibitory binding pocket in human AchE (Figure 1. b).

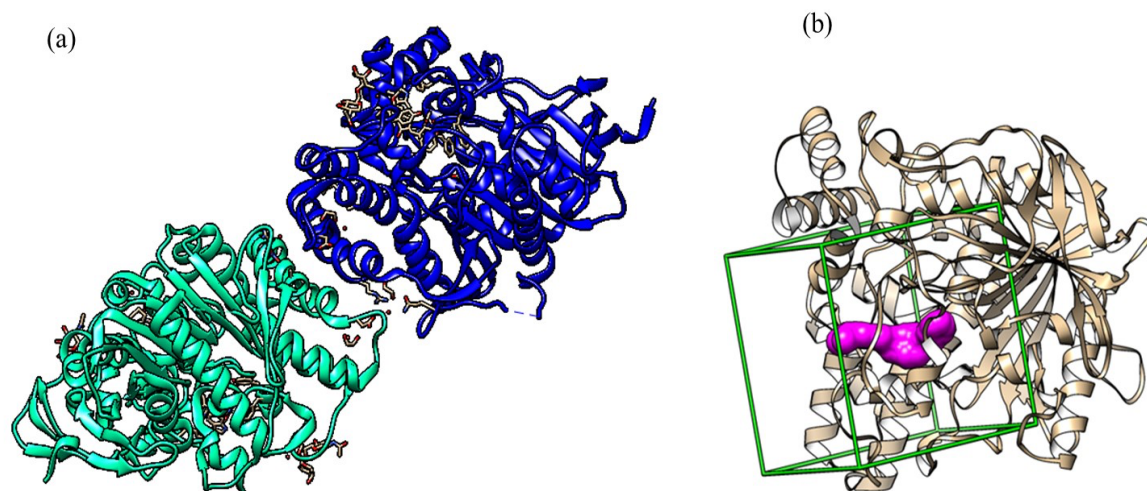


**Figure 1.** The crystal structure of human 4EY7. a) displaying the dimeric protein using the Chimera program b) representation of the active site in the crystal structure (4EY7\_E20).

Y337 which is a particularly flexible amino acid has been defined as the “swinging gate” of the active site that is pocketed upon donepezil binding [20]. Hydrophobic interactions, hydrogen bonds and  $\pi$ -stacking interactions play an important role in this binding. Hydrogen bonding (F295), hydrophobic interactions (W86, Y337, Y341, F338) and  $\pi$ -stacking (W286, W86, Y341) interactions play important roles in the binding of donepezil ligand to human AChE. Especially Y337, Y341, W286 and W86 amino acids draw attention in our study as well as in the 4EY7 crystal.

The interactions of rivastigmine, galantamine, tacrine, quercetin and genistein, which are very important drug substances using in the treatment of Alzheimer's, with human AChE protein were comparatively modeled. The docking poses of ligands in the catalytic site were very well superimposed with docking scores -7.8, -8.7, -8.6, -9.9 ve -9.3, kcal/mol respectively (Table 1). The binding energy of each ligand was calculated as -91.9, -111.0, -78.9, -119.2 and -108.4 (Table 2), respectively.

**Table 1.** Binding affinity of different ligands to the protein molecule, RMSD lower bound and RMSD upper bound\*.

DB Code	Name	$\Delta G$ kcal/mol	RMSD l.b	RMSD u.b
DB00989	rivastigmine	-7.8	2.177	6.769
DB00674	galantamin	-8.7	3.373	5.815
DB00382	tacrine	-8.6	1.456	2.795
DB04216	quercetin	-9.8	6.909	10.285
DB01645	genistein	-9.3	1.991	7.649

\* The predicted binding affinity is in kcal/mol (Energy). Root Mean Square (RMSD) values are calculated based on the best mode. The rmsd l.b (RMSD lower bound) and rmsd u.b (RMSD upper bound) metrics differ based on the matching of atoms in the distance calculation.

**Table 2.** Binding energy of ligands with protein molecule\*.

Ligand molecule	Binding energy (kcal / mol)
rivastigmine	-91.85
galantamin	-110.97
tacrine	-78.95
quercetin	-119.23
genistein	-108.35

\*Ligands were pre-screened with the IgemDock software. Binding energies of ligands are given in the table. quercetin is found as a complex in the crystal structure of recombinant human acetylcholinesterase.

These results show that quercetin is more effective than all currently known and tested ligands. When the protein-ligand bonds of all other ligands are examined in detail there are hydrogen bonding, hydrophobic and  $\pi$ -stacking interactions in other ligands as in 4EY7\_E20. All ligands examined in this study interact approximately 5 to 8 amino acids in the active site of the 4EY7 receptor (Figure 2).

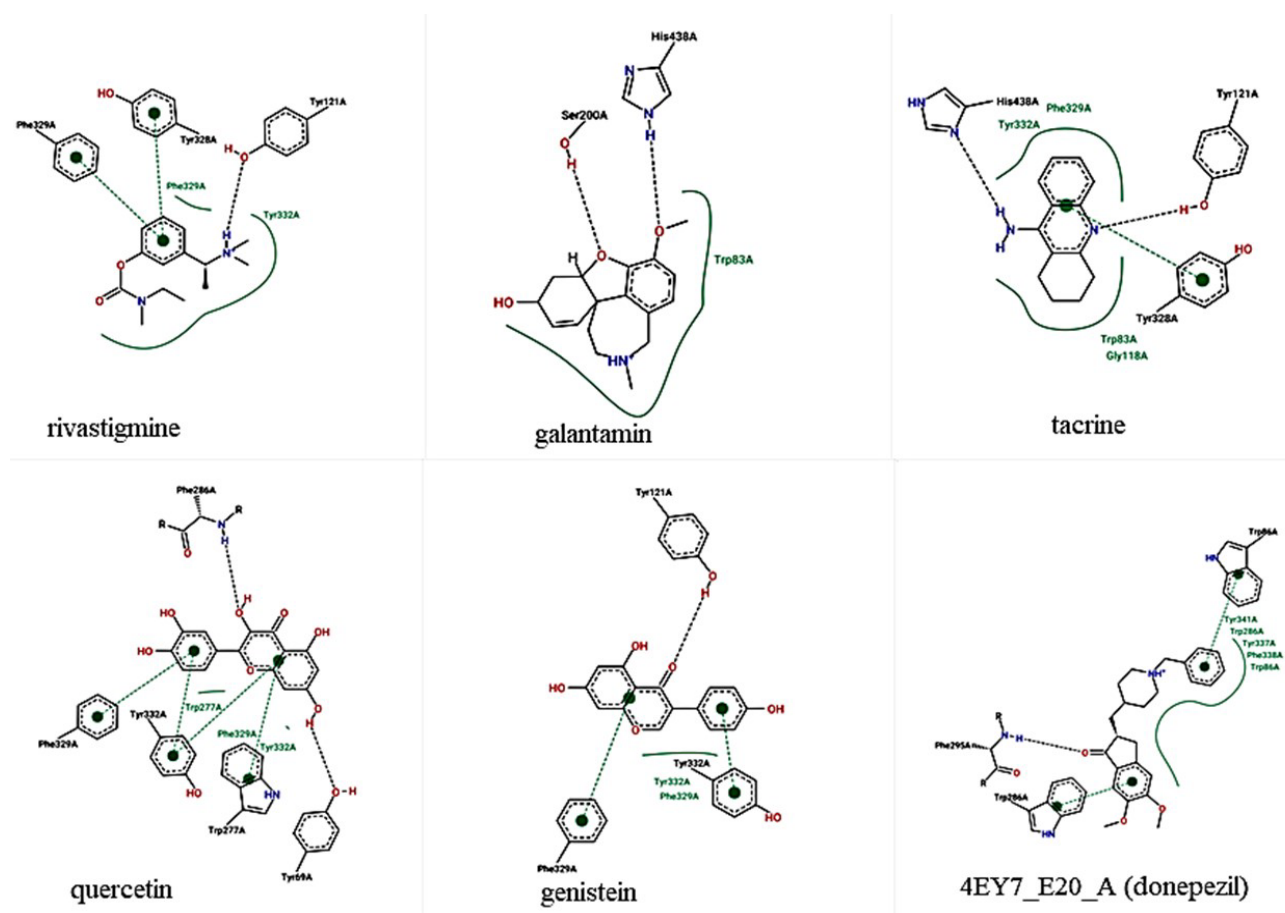


Figure 2. Interactions of protein and ligands

The interactions, bond types and the important amino acids in bonding can be expressed as follows. The case of binding of quercetin to human AChE, hydrogen bonds Y121, S284, F286, hydrophobic interactions Y121, F288, Y332 and W277, Y332  $\pi$ -stacking interactions play important roles. G118, Y121, S200 hydrogen bonds, W83, F329, Y332 hydrophobic interactions and W328  $\pi$ -stacking interactions were observed for rivastigmine. G117, G119, Y130, E199, S200 hydrogen bonds and W83, Y121, F288 hydrophobic forces play a role in the interaction between galantamine-AChE. Y121, H438 hydrogen bonds and W83, Y328, F329, Y332 hydrophobic interactions were noted in our tacrine-AChE modeling studies. G118, Y121, H438 hydrogen bonds, TRP277, F329, Y332 hydrophobic interactions and Y328, Y332  $\pi$ -stacking interactions were observed for genistein-AChE.

The amino acid-ligand interactions demonstrated here also indicate that these five ligands have good inhibitor potential for AChE. When the binding of these five ligands was examined in detail, it was observed that the shortest hydrogen bond distances, (H-A) of 2.87 Å, 3.05 Å, and 1.96 Å, were present in the binding of quercetin. In the original x-ray structure, the same hydrogen bond distance for donepezil was reported to be 1.99 Å. In addition, the lowest hydrogen bond distance in donepezil was 1.99 Å in the amino acid phenylalanine while this value was calculated as 1.96 Å in the same amino acid in quercetin. Therefore, this may indicate that quercetin binding may be stronger. Similarly, it has been demonstrated in the literature that the hydrogen bond strength which is responsible for the stability of the protein, plays an important role in the binding of flavonoids to AChE [21].

The molecular properties important for the pharmacokinetics of drug candidate molecules in the human body, including absorption, distribution, metabolism and excretion (ADME) were also investigated [22]. Table 3 presents Lipinski's five rules for assessing drug similarity and defining molecular properties. The physicochemical properties of the analyzed molecules fully comply with the Lipinski rule. The cell permeability, blood-brain barrier penetration as well as total polar surface area (TPSA) ( $\leq 140$ ) are within acceptable limits. A bioavailability value of 0.55 is critical for an oral drug. These calculations show promise for genistein and especially quercetin as pharmacological agents like galantamine, rivastigmine and tacrine.

**Table 3.** ADME profiles of potential drug derivatives.

Compounds	MW	Num.Rot. B.	H-Ac	H-Don	TPSA (Å <sup>2</sup> )	Con. Log P	Bioav. Score	LD50 (mg base/kg)	M	C	R
rivastigmine	250.34	6	3	0	32.78	2.34	0.55	5.6 (ma)*, 13.8 (fm)	-Not**	- Not***	-Not****
galantamin	287.35	6	4	1	41.93	1.91	0.55	-	NC	NC	NC
tacrine	198.26	0	1	1	38.91	2.59	0.55	5.2 [23]	-	-	-
quercetin	302.24	1	7	5	131.36	1.23	0.55	100-160 [24]	NA	NA	NA
genistein	270.24	1	5	3	90.90	2.04	0.55	2000 [25]	NH	NH	NH

\*M: Mutagenicity, C: Carcinogenicity, R: Reproductive Toxicity, (ma): male, (fm): female, NC: Not classified, NA: Not available (Human), NH: No hazard *in vivo* [26].

\*\*It was not mutagenic in *in vitro* tests for gene mutations and primary DNA damage.

\*\*\*No evidence of carcinogenicity was found in oral and topical studies in mice and in oral study in rats at the maximum tolerated dose.

\*\*\*\*Oral studies in pregnant rats and rabbits with dose levels up to 2.3 mg base/kg/day gave no indication of teratogenic potential on the part of rivastigmine.

Mutagenicity, carcinogenicity and reproductive toxicity values are summarized in Table 3 and no adverse events were observed in these values. In ADME results, quercetin with the highest hydrogen acceptor number 7 and the highest hydrogen donor number 5 showed the excess of hydrogen bonding here and supported the docking result.

The molecular dynamics simulation studies were summarized in Figure 3 and Figure 4. The B factor graphs reveal a comparison between the NMA (Normal Mode Analysis) and the PDB field of the complex. According to molecular dynamic simulations results the deformability and B factor figures reflect the mobility profiles of the docked proteins. The highest peaks in the deformability and B-factors of the quercetin-AChE complex represent regions of high deformability (Figure 3 a, b).

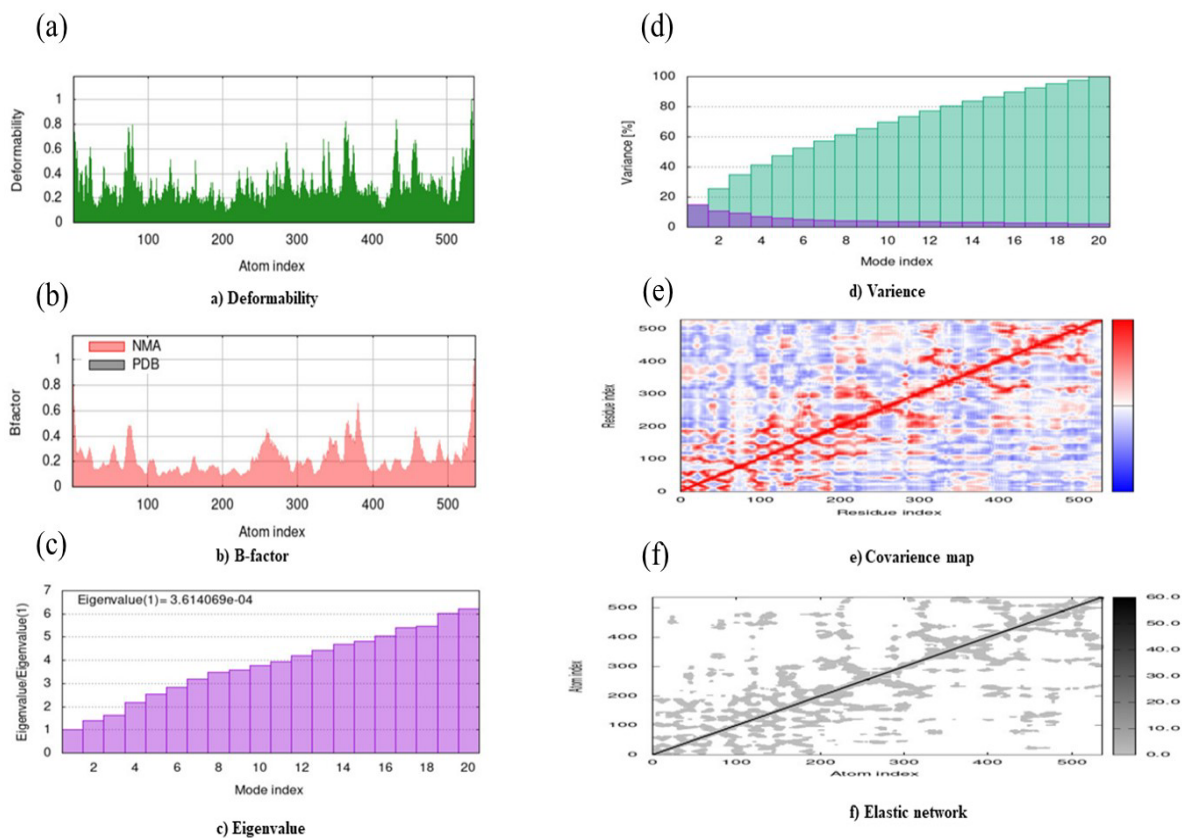


**Figure 3.** Outputs of molecular dynamics simulations in iMODS for quercetin-AChE complex. a) deformability and b) B-factor plot; c) eigenvalue and d) variance plot; e) covariance map; and f) elastic network model.

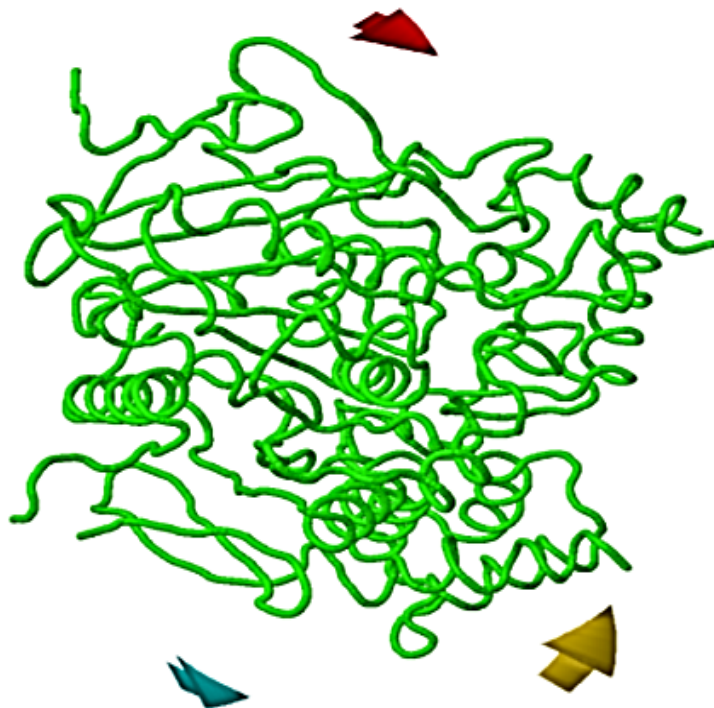


**Figure 4.** Molecular mobility assessed by NMA of the docked proteins. The three coloured affine arrows showed the mobility.

The eigenvalue and variance plot show an inverse relationship with the normal mode. The eigenvalue and variance graphs of the quercetin-AChE complex are shown in Figure 5 c and d. When examining the graph of variance of quercetin with protein, the cumulative variance is represented by green shaded bars, while the individual variance is represented by purple shaded bars. The eigenvalue of the complex calculated with iMod was found to be  $3,614069e^{-0.4}$ . The covariance map of the quercetin-AChE complex reveals the correlation between the residues of that complex. The blue color in the matrix indicates anticorrelation between the residues, while the red color indicates a good correlation. Also, white color reflects uncorrelated motion (Figure 3 e). When the relationship between atoms is examined on the elastic map, it can be said that the darker gray portions indicate the stiffer parts in Figure 3 f. The covariance matrices and elastic maps gave reasonable values.

### 3. CONCLUSION

Molecular docking and dynamic simulation studies provide a better understanding of quercetin interactions at the intermolecular level with the protein involved in Alzheimer's disease. The emerging findings highlight an important aspect of quercetin therapeutic potential.

### 4. MATERIALS AND METHODS

#### 4.1. Identification and Selection of Target Protein and Ligands

Human acetylcholinesterase (AChE) is an important target for therapeutic drugs [27]. The crystallographic structure of the E2O (Donepezil) bound 4EY7 (Acetylcholinesterase) protein was downloaded from the Protein Data Bank.

In addition to phytochemicals such as quercetin and genistein which are used to slow the onset and progression of Alzheimer's disease, the main drug class currently used for the treatment of Alzheimer's disease, AChE-Is (rivastigmine, galantamine and donepezil) have also been chosen as ligands. Unlike these ligands, tacrine is not included in the treatment due to its hepatotoxicity.

#### 4.2. Preparation of Protein and Ligands

The protein was saved in pdb file and the bound ligands and water molecules were deleted from original 3D structure [28, 29]. Polar hydrogen atoms and charges were added to the protein and saved in Mol2 file. SMILE screened ligand notations were copied from PubChem. Energy minimization is done using build structure tool in Chimera program. Ligands prepared in Mol2 file were made ready for docking.

#### 4.3. Final Docking with UCSF Chimera (1.16) and AutoDock Vina

The ligand molecule was imported in the output file saved as pdbqt. By entering the previously determined active site coordinates, AutoDock Vina was run using the command prompt and the results were analyzed [30].

#### 4.4. Grid Box Preparation

The active region used while docking was found by averaging the x, y, z coordinates of E2O which is bound to 4EY7 in the crystallographic structure (Table 4). The search area for the grid box is taken as  $30*30*30^*$  [31]. The experimental procedures should be described in sufficient detail to enable others to repeat the experiments. Names of products and manufacturers (with locations) should be supplied for all mentioned equipment, instruments, chemicals, etc. Brand names may be used only once in the manuscript. For example; you can mention that "XYZ® tablets containing Esomeprazole (Formulation A) were generously provided by ABC Pharmaceuticals" in Materials and Methods section. However, in other parts of the manuscript, it must be mentioned as "commercial tablets containing Esomeprazole" or Formulation A, not XYZ® tablets.

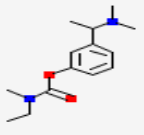
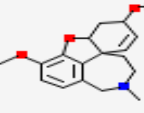
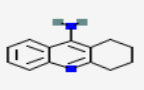
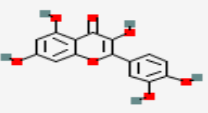
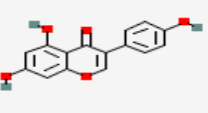
**Table 4.** Coordinate calculation of ligand E20 in chain 4EY7-A

HETATM	8423	C1	E20	A	604	-18.530	-41.928	24.258
HETATM	8424	C2	E20	A	604	-18.970	-41.862	25.566
HETATM	8425	C3	E20	A	604	-18.125	-42.222	26.615
HETATM	8426	C4	E20	A	604	-16.817	-42.659	26.338
HETATM	8427	C5	E20	A	604	-16.370	-42.740	25.037
HETATM	8428	C6	E20	A	604	-17.234	-42.369	23.979
HETATM	8429	C7	E20	A	604	-14.962	-43.221	24.996
HETATM	8430	C8	E20	A	604	-14.502	-43.478	26.419
HETATM	8431	C9	E20	A	604	-15.710	-43.107	27.282
HETATM	8432	C10	E20	A	604	-13.970	-44.894	26.642
HETATM	8433	C11	E20	A	604	-12.925	-44.965	27.776
HETATM	8434	C12	E20	A	604	-13.505	-44.756	29.141
HETATM	8435	C13	E20	A	604	-12.529	-44.933	30.274
Coordinates						<b>-15.704</b>	<b>-43.318</b>	<b>26.486</b>

#### 4.5. Software Used

Windows 10 is used as the Microsoft operating system. UCSF Chimera (1.16) program was used for docking with AutoDock Vina software [32]. AutoDock Vina, which is widely used for molecular docking simulations, is hosted by The Scripps Research Institute (USA) [32, 33]. Protein Data Bank (rcsb) and PubChem were used for protein and chemical structures (ligands), respectively (Table 5). IgemDOCK V2.1 was preferred for pre-scoring elimination of ligands. Plip-tool and proteins plus software were used for the bonds and distances between protein and ligands [34, 35].

**Table 5.** Structure of ligands

Structure	Ligand	PubChem ID
	rivastigmine	CID: 5077
	galantamin	CID: 3449
	tacrine	CID: 1935
	quercetin	CID: 5280343
	genistein	CID: 5280961

#### 4.6. In sico ADME properties

Examining the ADME properties of any molecule reveals their potential for becoming a drug. To calculate the biochemical and pharmacokinetics properties of the selected molecules used the SwissADME online server [36]. The SwissADME server was operated to exactly comment the biochemical properties, and



the molecules analyzed had to follow Lipinski's 5 rules. In Table 3 properties of the ligands and their calculated ADME parameters such as molecular weights (MW), number of hydrogen bond donors (H-Don) and acceptors (H-Ac), octanol-water partition coefficient (log P) and topological polar surface area (TPSA) values are provided.

#### 4.7. Molecular dynamic simulations

iMod program package was used for modelling, imaging and 3D data analysis [37]. Based on the docking results, molecular dynamics analysis studies were conducted on the selected docked complex with the lowest energy value under conditions of 300 K temperature and 1 atm constant pressure.

**Acknowledgements:** The author is very thankful to University of Health Sciences for their contribution to the completion of this research.

**Author contributions** Concept – Ş.K.; Design – Ş.K.; Analysis and Interpretation – Ş.K.; Literature Search – Ş.K.; Writing – Ş.K. Concept – H.A.; Design – H.A.; Analysis and Interpretation – H.A.; Literature Search – H.A.; Writing – H.A.

**Conflict of interest statement:** "The authors declared no conflict of interest" in the manuscript.

#### REFERENCES

- [1] D'Onofrio G, Sancarlo D, Ruan Q, Yu Z, Panza F, Daniele A, Greco A, Seripa D. Phytochemicals in the Treatment of Alzheimer's Disease: A Systematic Review. *Curr Drug Targets*. 2017;18(13):1487-1498. <https://doi.org/10.2174/1389450117666161102121553>
- [2] Marucci G, Buccioni M, Ben DD, Lambertucci C, Volpini R, Amenta F. Efficacy of acetylcholinesterase inhibitors in Alzheimer's disease. *Neuropharmacology*. 2021; 1;190:108352. <https://doi.org/10.1016/j.neuropharm.2020.108352>
- [3] Kim MH, Kim SH, Yang WM. Mechanisms of action of phytochemicals from medicinal herbs in the treatment of Alzheimer's disease. *Planta Med*. 2014 Oct;80(15):1249-58. <https://doi.org/10.1055/s-0034-1383038>
- [4] Al-Shabib NA, Khan JM, Malik A, Alsenaidy A, Rehman MT, AlAjmi MF, Alsenaidy AM, Husain FM, Khan RH. Molecular insight into binding behavior of polyphenol (rutin) with beta lactoglobulin: Spectroscopic, molecular docking and MD simulation studies. 2018; 269: 511-520. <https://doi.org/10.1016/j.molliq.2018.07.122>
- [5] Kelleci Çelik F, Karaduman G. In silico QSAR modeling to predict the safe use of antibiotics during pregnancy. *Drug Chem Toxicol*. 2022 Aug 22:1-10. <https://doi.org/10.1080/01480545.2022.2113888>
- [6] Shah MS, Najam-Ul-Haq M, Shah HS, Farooq Rizvi SU, Iqbal J. Quinoline containing chalcone derivatives as cholinesterase inhibitors and their in silico modeling studies. *Comput Biol Chem*. 2018 Oct;76:310-317. <https://doi.org/10.1016/j.compbiolchem.2018.08.003>
- [7] Singh SP, Gupta D. Discovery of potential inhibitor against human acetylcholinesterase: a molecular docking and molecular dynamics investigation. *Comput Biol Chem*. 2017 Jun;68:224-230. <https://doi.org/10.1016/j.compbiolchem.2017.04.002>
- [8] Abbasi MA, Hassan M, Ur-Rehman A, Siddiqui SZ, Hussain G, Shah SAA, Ashraf M, Shahid M, Seo SY. 2-Furoic piperazide derivatives as promising drug candidates of type 2 diabetes and Alzheimer's diseases: In vitro and in silico studies. *Comput Biol Chem*. 2018 Dec;77:72-86. <https://doi.org/10.1016/j.compbiolchem.2018.09.007>
- [9] Manouchehrizadeh E, Mostoufi A, Tahanpesar E, Fereidoonhezad M. Alignment-independent 3D-QSAR and molecular docking studies of tacrine-4-oxo-4H-Chromene hybrids as anti-Alzheimer's agents. *Comput Biol Chem*. 2019 Jun;80:463-471. <https://doi.org/10.1016/j.compbiolchem.2019.05.010>
- [10] Pourshojaei Y, Abiri A, Eskandari R, Dourandish F, Eskandari K, Asadipour A. Synthesis, biological evaluation, and computational studies of novel fused six-membered O-containing heterocycles as potential acetylcholinesterase inhibitors. *Comput Biol Chem*. 2019 Jun;80:249-258. <https://doi.org/10.1016/j.compbiolchem.2019.04.004>
- [11] de Souza LG, Moraes PF, Leão RAC, Costa PRR, Soares RO, Pascutti PG, Figueroa-Villar JD, Rennó MN. Theoretical studies and NMR assay of coumarins and neoflavanones derivatives as potential inhibitors of acetylcholinesterase. *Comput Biol Chem*. 2020 May 29;87:107293. <https://doi.org/10.1016/j.compbiolchem.2020.107293>
- [12] Kumar V, Saha A, Roy K. In silico modeling for dual inhibition of acetylcholinesterase (AChE) and butyrylcholinesterase (BuChE) enzymes in Alzheimer's disease. *Comput Biol Chem*. 2020 Oct;88:107355. <https://doi.org/10.1016/j.compbiolchem.2020.107355>

- [13] Bousada GM, de Sousa BL, Furlani G, Agrizzi AP, Ferreira PG, Leite JPV, Mendes TAO, Varejão EVV, Pilau EJ, Dos Santos MH. Tyrosol 1,2,3-triazole analogues as new acetylcholinesterase (AChE) inhibitors. *Comput Biol Chem.* 2020 Oct;88:107359. <https://doi.org/10.1016/j.compbiolchem.2020.107359>
- [14] Anwar F, Saleem U, Ahmad B, Ashraf M, Rehman AU, Froeyen M, Kee LY, Abdullah I, Mirza MU, Ahmad S. New naphthalene derivative for cost-effective AChE inhibitors for Alzheimer's treatment: In silico identification, in vitro and in vivo validation. *Comput Biol Chem.* 2020 Dec;89:107378. <https://doi.org/10.1016/j.compbiolchem.2020.107378>
- [15] Morris GM and Lim-Wilby M. Molecular Docking. In *Molecular modeling of proteins.* Humana Press. 2008:365-382. [https://doi.org/10.1007/978-1-59745-177-2\\_19](https://doi.org/10.1007/978-1-59745-177-2_19)
- [16] Çelik S, Demirag AD, Coşgun AO, Özel A, Akyüz S. Computational Investigation of the Interaction Mechanism of Some anti-Alzheimer Drugs with the Acetylcholinesterase Enzyme. *OJN.* 2023; 8(1): 11-21. <https://doi.org/10.56171/ojn.1109606>
- [17] Ruangritchankul S, Chantharit P, Srisuma S, Gray LC. Adverse Drug Reactions of Acetylcholinesterase Inhibitors in Older People Living with Dementia: A Comprehensive Literature Review. *Ther Clin Risk Manag.* 2021 Sep 4;17:927-949. <https://doi.org/10.2147/tcrm.s323387>
- [18] Cheung J, Rudolph MJ, Burshteyn F, Cassidy MS, Gary EN, Love J, Franklin MC, Height JJ. Structures of human acetylcholinesterase in complex with pharmacologically important ligands. *J Med Chem.* 2012 Nov 26;55(22):10282-86. <https://doi.org/10.1021/jm300871x>
- [19] Xu Y, Colletier JP, Weik M, Jiang H, Moulton J, Silman I, Sussman JL. Flexibility of aromatic residues in the active-site gorge of acetylcholinesterase: X-ray versus molecular dynamics. *Biophys J.* 2008 Sep;95(5):2500-11. <https://doi.org/10.2478/s11696-013-0354-4>
- [20] Kumar B, Thakur A, Dwivedi AR, Kumar R, Kumar V. Multi-Target-Directed Ligands as an Effective Strategy for the Treatment of Alzheimer's Disease. *Curr Med Chem.* 2022;29(10):1757-1803. <https://doi.org/10.2174/1875533xmtel1dnjei3>
- [21] Xie Y, Yang W, Chen X, Xiao J. Inhibition of flavonoids on acetylcholine esterase: binding and structure-activity relationship. *Food Funct.* 2014 Oct;5(10):2582-9. <https://doi.org/10.1039/c4fo00287c>
- [22] Lipinski CA. Lead- and drug-like compounds: the rule-of-five revolution. *Drug Discov Today Technol.* 2004 Dec;1(4):337-41. <https://doi.org/10.1016/j.ddtec.2004.11.007>
- [23] Misik J, Nepovimova E, Pejchal J, Kassa J, Korabecny J, Soukup O. Cholinesterase Inhibitor 6-Chlorotacrine - In Vivo Toxicological Profile and Behavioural Effects. *Curr Alzheimer Res.* 2018;15(6):552-560. <https://doi.org/10.2174/1567205015666171212105412>
- [24] Sullivan M, Follis RH Jr, Hilgartner M. Toxicology of podophyllin. *Proc Soc Exp Biol Med.* 1951 Jun;77(2):269-72. <https://doi.org/10.3181/00379727-77-18746>
- [25] Michael McClain R, Wolz E, Davidovich A, Pfannkuch F, Edwards JA, Bausch J. Acute, subchronic and chronic safety studies with genistein in rats. *Food Chem Toxicol.* 2006 Jan;44(1):56-80. <https://doi.org/10.1016/j.fct.2005.05.021>
- [26] Michael McClain R, Wolz E, Davidovich A, Bausch J. Genetic toxicity studies with genistein. *Food Chem Toxicol.* 2006 Jan;44(1):42-55. <https://doi.org/10.1016/j.fct.2005.06.004>
- [27] Cheung J, Rudolph MJ, Burshteyn F, Cassidy MS, Gary EN, Love J, Franklin MC, Height JJ. Structures of human acetylcholinesterase in complex with pharmacologically important ligands. *J Med Chem.* 2012 Nov 26;55(22):10282-6. <https://doi.org/10.1021/jm300871x>
- [28] Pettersen EF, Goddard TD, Huang CC, Couch GS, Greenblatt DM, Meng EC, Ferrin TE. UCSF Chimera--a visualization system for exploratory research and analysis. *J Comput Chem.* 2004 Oct;25(13):1605-12. <https://doi.org/10.1002/jcc.20084>
- [29] Goddard TD, Huang CC, Ferrin TE. Visualizing density maps with UCSF Chimera. *J Struct Biol.* 2007 Jan;157(1):281-7. <https://doi.org/10.1016/j.jsb.2006.06.010>
- [30] Butt SS, Badshah Y, Shabbir M, Rafiq M. Molecular Docking Using Chimera and AutoDock Vina Software for Nonbioinformaticians *JMIR Bioinform Biotech* 2020;1(1):e14232 <https://doi.org/10.2196/preprints.14232>
- [31] Del Águila Conde M, Febbraio F. Risk assessment of honey bee stressors based on in silico analysis of molecular interactions. *EFSA J.* 2022 Dec 14;20(Suppl 2):e200912. <https://doi.org/10.2903/j.efsa.2022.e200912>
- [32] Ferreira LG, Dos Santos RN, Oliva G, Andricopulo AD. Molecular docking and structure-based drug design strategies. *Molecules.* 2015 Jul 22;20(7):13384-421. <https://doi.org/10.3390/molecules200713384>
- [33] Sandeep G, Nagasree KP, Hanisha M, Kumar MM. AUdocker LE: A GUI for virtual screening with AUTODOCK Vina. *BMC Res Notes.* 2011 Oct 25;4:445. <https://doi.org/10.1186/1756-0500-4-445>

- [34] Adasme MF, Linnemann KL, Bolz SN, Kaiser F, Salentin S, Haupt VJ, Schroeder M. PLIP 2021: expanding the scope of the protein-ligand interaction profiler to DNA and RNA. *Nucleic Acids Res.* 2021 Jul 2;49(W1):W530-W534. <https://doi.org/10.1093/nar/gkab294>
- [35] Schöning-Stierand K, Diedrich K, Ehrh C, Flachsenberg F, Graef J, Sieg J, Penner P, Poppinga M, Ungethüm A, Rarey M. ProteinsPlus: a comprehensive collection of web-based molecular modeling tools. *Nucleic Acids Res.* 2022 Jul 5;50(W1):W611-W615. <https://doi.org/10.1093/nar/gkac305>
- [36] Daina A, Michielin O, Zoete V. SwissADME: a free web tool to evaluate pharmacokinetics, drug-likeness and medicinal chemistry friendliness of small molecules. *Sci Rep.* 2017 Mar 3;7:42717. <https://doi.org/10.1038/srep42717>
- [37] Kremer JR, Mastrorade DN, McIntosh JR. Computer visualization of three-dimensional image data using IMOD. *J Struct Biol.* 1996 Jan-Feb;116(1):71-6. <https://doi.org/10.1006/jsbi.1996.0013>